Density functional theory and resonance Raman investigation of the ultraviolet electronic excited states of CF2I2

ARTICLE *in* CHEMICAL PHYSICS LETTERS · JANUARY 2000

Impact Factor: 1.9 · DOI: 10.1016/S0009-2614(99)01353-6

2 AUTHORS:

Xuming Zheng
Zhejiang Sci-Tech University
109 PUBLICATIONS **1,262** CITATIONS
SEE PROFILE

David Lee Phillips
The University of Hong Kong
345 PUBLICATIONS **7,054** CITATIONS
SEE PROFILE

21 January 2000

ELSEVIER

Chemical Physics Letters 316 (2000) 524–530

CHEMICAL PHYSICS LETTERS

www.elsevier.nl/locate/cplett

Density functional theory and resonance Raman investigation of the ultraviolet electronic excited states of CF_2I_2

Xuming Zheng, David Lee Phillips *

Department of Chemistry, University of Hong Kong, Pokfulam Road, Hong Kong, China

Received 24 September 1999; in final form 15 November 1999

Abstract

We report density functional theory calculation results that examine the ultraviolet electronic transitions of CF_2I_2 and CH_2I_2. We make preliminary assignments of several transitions to the ultraviolet absorption spectra of CF_2I_2 and CH_2I_2. We compare our present results to previous experimental and computational work. We also examine the molecular orbitals involved in the electronic transitions assigned to the absorption spectra.

1. Introduction

Ultraviolet photoexcitation of CF_2I_2 and CH_2I_2 molecules leads primarily to cleavage of one C–I bond for CH_2I_2 but wavelength-dependent competition between one C–I bond cleavage and two C–I bond cleavage reactions for CF_2I_2 [1–16]. Both CF_2I_2 and CH_2I_2 show no evidence for appreciable molecular I_2 elimination reactions from 220 to 400 nm. CH_2I_2 photodissociation from 200 to 400 nm gives mostly the $CH_2I + I$ (or I^*) dissociation channels [1,2,4–6,8–10]. Molecular beam studies of CF_2I_2 photodissociation indicate that photoexcitation from 308 to 352 nm results in mostly the $CF_2I + I$ (or I^*) dissociation channel while 248 nm excitation results in mostly the $CF_2 + I + I$ (or I^*) three-body dissociation channel [11,12]. An ultrafast spectroscopy experiment with 266 nm excitation of CF_2I_2 showed that CF_2I_2 initially forms a $[CF_2I_2]$ intermediate within ~ 30 fs which then dissociates with $\tau \approx 100$ fs into $CF_2 + I + I$ fragments [16]. The ultraviolet photodissociation reactions of CH_2I_2 and CF_2I_2 display significant differences although their absorption spectra are very similar and they have the same symmetry point group and the same two C–I bond chromophores. Resonance Raman investigations have been done to characterize the short-time photodissociation dynamics of several CH_2I_2 transitions in both the gas and solution phases [17–22].

The first absorption band of both CF_2I_2 and CH_2I_2 is near 300 nm and made up of several overlapping transitions [1,3,5,10,12]. The CH_2I_2 ultraviolet absorption band has been deconvoluted into four (or five) bands at 214, 249, 285, and 311 nm. A simple exciton model calculation was used to tentatively assign the 249, 285, and 311 nm bands to B_2/A_1, B_1, and B_1 transitions, respectively [1]. Similarly, the 249, 300, and 351 nm bands in the CF_2I_2 ultraviolet absorption have been tentatively assigned to three B_1 states based on molecular beam anisotropy parameters [12]. However, magnetic circular

* Corresponding author. Fax: +852-2857-1586; e-mail: philips@hkucc.hku.hk

0009-2614/00/$ - see front matter
PII: S0009-2614(99)01353-6

dichroism (MCD) experiments done for CH_2I_2 determined the two bands ~ 295 and ~ 276 nm correlate to B_1 and B_2 states with undetermined order and a weak shoulder ~ 313 nm that correlates to a nominally forbidden transition [3]. This discrepancy between the MCD results and those for the simple exciton model computations and molecular beam polarization experiments for CH_2I_2 remains to be resolved [1,3]. This uncertainty in the CH_2I_2 absorption band assignments may also have implications for the CF_2I_2 absorption band assignments that are based on the CH_2I_2 results and limited experimental data.

In this Letter, we report density functional theory (DFT) calculations of the electronic transition energies and oscillator strengths to examine the ultraviolet absorption bands of CH_2I_2 and CF_2I_2. We also report resonance Raman spectra of CH_2I_2 and CF_2I_2 and discuss the resonance Raman intensity patterns as a function of wavelength and their relationship to other experimental data. We compare our DFT calculation results to previous work on CH_2I_2 and CF_2I_2. We find good agreement between our current results and those of the MCD experiments done for CH_2I_2. We present preliminary assignments for the ultraviolet absorption transitions based on the DFT computations, resonance Raman spectra, and previously reported experimental results.

2. Experiment and calculations

Sample solutions of CF_2I_2 (99%-custom synthesis by Strem Chemicals) in cyclohexane solution were prepared with 0.08–0.10 M concentration for the resonance Raman experiments. The sample solution concentrations were between 0.15 and 0.20 M for CH_2I_2 (99%-Aldrich) in methanol solvent. The resonance Raman experimental apparatus and methods have been reported previously [19,20] and only a short description will be given here. The harmonic and hydrogen Raman shifted lines of a pulsed Nd:YAG laser were used to excite a flowing liquid sample in the resonance Raman experiments using a $\sim 135°$ backscattering geometry. The Raman scattered light was collected with reflective optics and imaged through a depolarizer and entrance slit to a 0.5 m spectrograph which imaged the light onto a liquid-nitrogen-cooled CCD detector. The CCD detector acquired the Raman light for ~ 120–600 s before being read out to an interfaced PC computer for further analysis. Approximately ten to thirty readouts were added together with a corresponding number of dark scans subtracted to give the resonance Raman spectrum. The known vibrational frequencies of the solvent and Hg emission lines were used to calibrate the Raman shifts of the spectra in cm^{-1} units. A spectrum of an intensity calibrated deuterium lamp was used to correct the spectra for the wavelength dependence of the detection system response. The resonance Raman spectra were also corrected for any remaining sample reabsorption of the Raman signal and solvent subtracted.

All the DFT calculations reported here made use of the GAUSSIAN 98 program suite [23]. Complete geometry optimization were done analytically at the B3LYP/3-21G* levels of theory for the ground state [24]. The electronic transitions were computed using DT(RPA) (time-dependent DFT at random phase approximation) [25] (RPA/3-21G*) level of theory.

3. Results and discussion

Fig. 1 displays the absorption spectrum of CF_2I_2 in cyclohexane solution. The dashed lines in Fig. 1

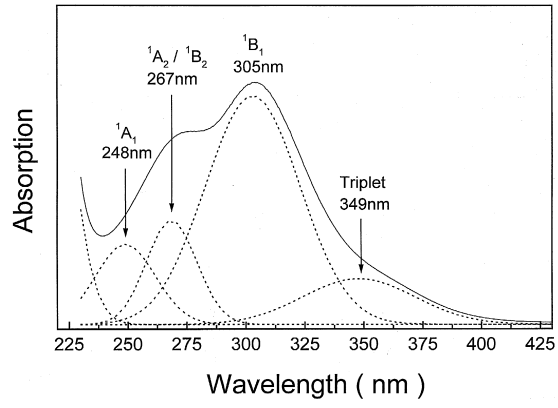

Fig. 1. Absorption spectrum of CF_2I_2 in cyclohexane solution. The dashed lines display a gaussian deconvolution of the experimental spectrum and the main transitions have been labeled with their positions and preliminary assignments (see discussion in text).

are a simple gaussian deconvolution of the absorption spectrum. The absorption band appears to have three subbands at ~270, 306, and 362 nm and can be deconvoluted into four transitions (at 248, 267, 305, and 349 nm, respectively). In order to help make preliminary assignments to these four possible transitions, we have performed DFT calculations of the electronic transitions and taken a resonance Raman partial excitation profile. Fig. 2 presents an overview of the resonance Raman spectra obtained for 341.5, 309.1, 266.0, 273.9, and 239.5 nm excitation. Table 1 lists the RPA/B3LYP/3-21G* calculated transition energies with their oscillator strengths

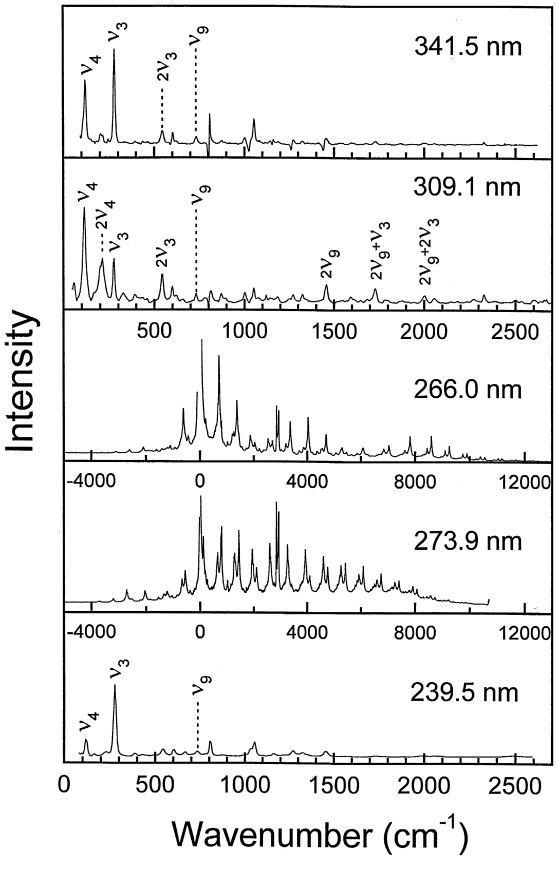

Fig. 2. Resonance Raman/fluorescence spectra of CF_2I_2 in cyclohexane solution acquired with excitation wavelengths of 341.5, 309.1, 266.0, 273.9 and 239.5 nm. The spectra have been intensity corrected and solvent subtracted. The assignments of some of the larger Raman bands are labeled (ν_4 = nominal I–C–I bend, ν_3 = nominal I–C–I symmetric stretch, and ν_9 = nominal I–C–I antisymmetric stretch).

and the experimental absorption bands for CF_2I_2. We also display similar results for CH_2I_2 since it is useful for comparison purposes.

Since the ultraviolet absorption of CF_2I_2 has some similarity to that of CH_2I_2, we shall first consider the better characterized CH_2I_2 absorption. The absorption of CH_2I_2 in the ultraviolet has been decomposed into four (or five) bands at 214, 249, 285, and 311 nm [1,17]. A simple exciton model [1] was used to assign these bands as follows: the 311 and 285 nm bands to B_1 states, the 249 nm band to B_2 and A_1 states, and the 214 nm band to an A_1 state. Molecular beam polarization results for CH_2I_2 appeared to support the assignment of the 311 and 285 nm bands to B_1 states [1]. However, magnetic circular dichroism (MCD) experiments by Gedanken and Rowe [3] indicated that the two bands ~296 and 276 nm correlate to B_1 and B_2 with undetermined order and the >310 nm shoulder correlates to a nominally forbidden transition. Fig. 3 presents resonance Raman spectra of CH_2I_2 obtained with excitation of 355 and 309.1 nm excitation and Table 1 shows the DFT results for the calculated electronic transitions for CH_2I_2. The 355 nm resonance Raman spectrum of CH_2I_2 is similar to those found for the weaker nominally forbidden Q transitions associated the A-band of iodoalkanes (which are mainly composed of the $^3Q_0$ transition – a parallel transition relative to the C–I bond) [26–32] but the 309.1 nm spectrum is significantly different with great enhancement of the B_1 symmetry I–C–I asymmetric mode ν_9 fundamental, overtones and combination bands. This suggests that the 309 nm region and the 355 nm region correspond to two distinctly different transitions. The DFT results of Table 1 indicate the assignments of the of experimental absorption band of CH_2I_2 is as follows: the shoulder above 320 nm is due to nominally forbidden triplet transitions (probably the $^3B_1$ transition ~347 nm), the 311 nm band is a $^1B_1$ transition, the 285 nm band arises from a $^1B_2$ transition, the 249 and 214 nm bands are due to $^1A_1$ transitions. Our DFT results (as well as the resonance Raman spectra) appear consistent with the assignments of the MCD experiments. There is a discrepancy between our results (and the MCD experiments) with the exciton model calculations and molecular beam experiments for the 285 nm absorption band assignment. The simple exciton model

Table 1
Comparison of experimental absorption transition energies with calculated values from density functional theory calculations for CF_2I_2 and CH_2I_2 in the ultraviolet region

CF_2I_2			CH_2I_2			Exciton
State	RPA/B3LYP calc.	expt.[a]	state	RPA/B3LYP calc.	expt.[b]	model[b]
$^1B_1$	294 nm ($f = 0.0123$)	305 nm	$^1B_1$	285 nm ($f = 0.0182$)	311 nm	$^1B_1$
$^1A_2$	276 nm ($f = 0.000$)	267 nm	$^1B_2$	262 nm ($f = 0.0027$)	285 nm	$^1B_1$
$^1B_2$	259 nm ($f = 0.0038$)	267 nm	$^1A_2$	248 nm ($f = 0.0000$)	249 nm	
$^1A_1$	250 nm ($f = 0.0016$)	248 nm	$^1A_1$	237 nm ($f = 0.0003$)	249 nm	$^1B_2/^1A_1$
$^1B_1$	184 nm ($f = 0.7974$)		$^1A_1$	160 nm ($f = 0.0169$)	214 nm	A_1
$^3B_1$	409 nm ($f = 0.000$)		$^3B_1$	347 nm ($f = 0.000$)		
$^3A_2$	366 nm ($f = 0.000$)		$^3B_2$	317 nm ($f = 0.000$)		
$^3B_2$	345 nm ($f = 0.000$)		$^3A_1$	312 nm ($f = 0.000$)		
$^3A_1$	338 nm ($f = 0.000$)		$^3A_2$	306 nm ($f = 0.000$)		
$^3B_1$	310 nm ($f = 0.000$)		$^3A_1$	248 nm ($f = 0.000$)		
$^3B_1$	266 nm ($f = 0.000$)		$^3B_1$	236 nm ($f = 0.000$)		

[a] This work. Gaussian deconvolution of experimental spectrum of Fig. 1.
[b] Values from Ref. [1].

calculations may not account for electron correlation effects very well compared to the DFT computations (which could still be improved upon with higher levels of theory and/or basis sets). However, it is not clear why there is a disagreement for the 285 nm band experimental results.

Since CF_2I_2 has the same point group and two similar C–I chromophores like CH_2I_2, one may expect the CF_2I_2 ultraviolet absorption spectra assignments are similar to those for CH_2I_2 [1,3,12]. However, the interaction of the two C–F chromophores with the two C–I chromophores in CF_2I_2 may not be negligible and could noticeably perturb the electronic spectra. Inspection of Fig. 2 shows that there are significant changes in the relative intensity patterns of the resonance Raman/fluorescence spectra for CF_2I_2 as one tunes the excitation wavelength. The differences in the 341.5 nm spectrum and the 309.1 nm spectrum are very similar to differences observed in the corresponding resonance Raman spectra of CH_2I_2: there appears to be a large enhancement of the B_1 I–C–I asymmetric stretch mode ν_9 fundamental, overtones and combination bands in the 309.1 nm spectra compared to the red-edge excitation in the 340–355 nm region (again indicating two distinct transitions). The DFT results in Table 1 for CF_2I_2 indicate that the 305 nm band is assigned to a $^1B_1$ transition and the 349 nm shoulder band is likely due to nominally forbidden triplet transitions. This is similar to the situation found for CH_2I_2. The resonance Raman spectra of CF_2I_2 in Fig. 2 for excitation at 266 and 273.9 nm have a large amount of CF_2 or other transient species fluorescence [33–35] as well as some CF_2I_2 resonance Raman intensity. Ultrafast spectroscopy experiments with 266 nm excitation of CF_2I_2 found that the CF_2I_2 initially forms an excited $[CF_2I_2]$ intermediate within ~ 30 fs and then dissociates with $\tau \approx 100$ fs

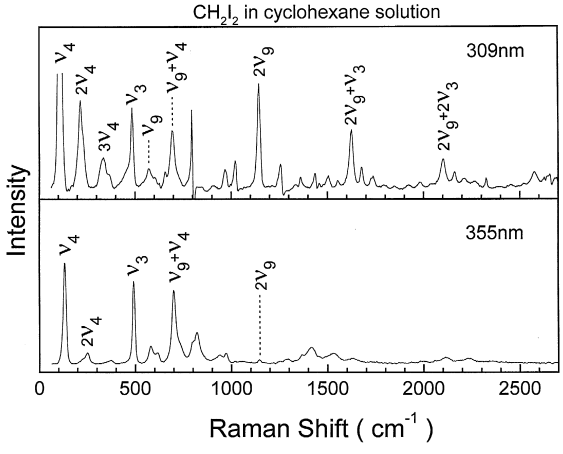

Fig. 3. Resonance Raman spectra of CH_2I_2 in methanol solution acquired with 309.1 and 355 nm excitation. The assignments of some of the larger Raman bands are labeled (ν_4 = nominal I–C–I bend, ν_3 = nominal I–C–C symmetric stretch, and ν_9 = nominal I–C–I antisymmetric stretch).

into CF_2, I and I_2 fragments with no evidence of a CF_2I fragment [16]. Molecular beam experiments with 351–248 nm excitation for CF_2I_2 exhibited competition between a $CF_2I + I$ product channel and a three-body $CF_2 + I + I$ product channel [11,12]. The two-body $CF_2I + I$ product channel is the predominant channel for the 352–308 nm excitation but the three-body $CF_2 + I + I$ product channel is predominant at 248 nm for photodissociation of CF_2I_2 [12]. This is consistent with our resonance Raman spectra of Fig. 2 which exhibit resonance Raman spectra for CF_2I_2 similar to CH_2I_2 from 309 to 355 nm (note both CF_2I_2 and CH_2I_2 have $CF_2I + I$ or $CH_2I + I$ as the predominant photodissociation channel in the 309–355 nm region) [1,2,4–6,8–10, 13] while the 266 and 273.9 nm CF_2I_2 spectra display CF_2 fluorescence consistent with the expected three-body dissociation channel in this region) [12,16] (this is somewhat fortuitous since CF_2 just happens to have an absorption band in the same region) [33–35].

In order to help better understand the photodissociation channel corresponding with the excited electronic states, we have examined the molecular orbitals involved in the most relevant electronic transitions. Fig. 4 shows six molecular orbitals from the DFT calculations associated with the electronic transitions assigned to the experimental absorption bands in Table 1 for CF_2I_2. Molecular orbitals 62 and 64 are the two σ_{C-I} bonding orbitals, orbitals 63 and 65 are the nonbonding orbitals populated by the two lone-pair of nonbonding 5p electrons of the two iodine atoms, and orbitals 66 and 67 are the two σ^*_{C-I} anti-bonding orbitals. The calculated $^1B_1$ transition (294 nm computed value assigned to the 305 nm experimental band) is associated with the transition of an electron in orbital 65 (nonbonding) to orbital 66 (σ^*_{C-I}). This gives a moderate weakening of the C–I bond order and the $^1B_1$ transition appears to correlate with one C–I bond cleavage. Similarly, the $^1B_2$ transition (calculated 259 nm assigned to the 267 nm experimental band) would also appear to correlate with one C–I bond cleavage (e.g., the $CF_2I + I$ (or I^*) channel). However, the $^1A_1$ transition (250 nm calculated and assigned to the 248 nm experimental band) and the $^1A_2$ (computed to be 276 nm and assigned to the 267 nm experimental band) transition are likely correlated to the $CF_2 + I + I$ channel since these transitions promote an electron from the σ_{C-I} bonding orbitals 62 or 64 to the σ^*_{C-I} antibonding orbital 66 to give a greater amount of reduction of the C–I bond order than the other allowed transitions. The three-body dissociation channel is not observed at excitation wavelengths above 250 nm for CH_2I_2 but can be observed up to 308 nm in CF_2I_2 (and becomes predominant below

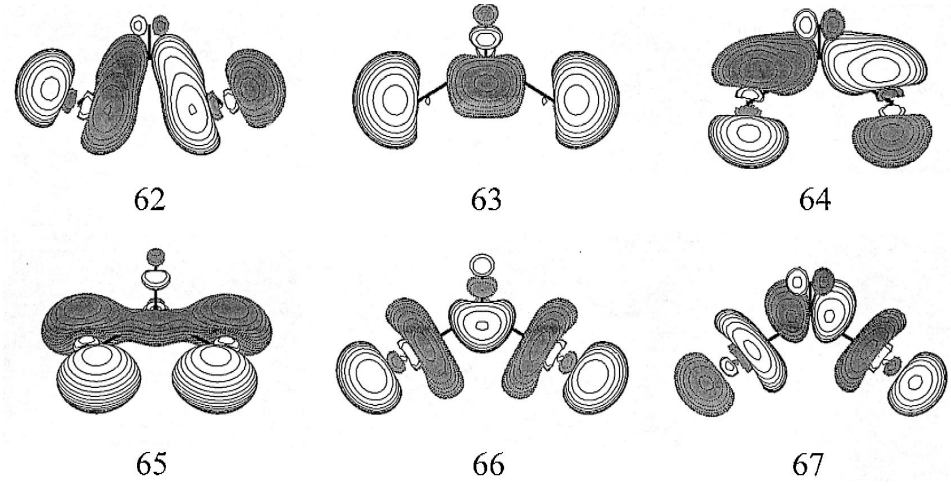

Fig. 4. Electron density contours for six CF_2I_2 molecular orbitals computed from RPA/B3LYP density functional theory calculations: orbitals 62 and 64 are the two σ_{C-I} bonding orbitals, orbitals 63 and 65 are the nonbonding orbitals populated by the two lone-pair of nonbonding 5P electrons of the two iodine atoms, and orbitals 66 and 67 are the two σ^*_{C-I} anti-bonding orbitals.

280 nm) [1,2,4–6,8–13,16]. Both CH_2I_2 and CF_2I_2 have $^1A_1$ transitions in the 250 nm region and the different thermochemistry toward C–I bond cleavage in both molecules is probably responsible for the different major dissociation channels for these molecules. The dissociation energy to break the first C–I bond is very similar for both CF_2I_2 and CH_2I_2 (~ 213 kJ/mol) but the total energy needed to break both C–I bonds is very different (~ 265 kJ/mol for CF_2I_2 and ~ 477 kJ/mol for CH_2I_2) [12]. This appears to make it easier for the three-body dissociation channel to take place at lower energies (or higher excitation wavelengths) for CF_2I_2 than for CH_2I_2. We note that these correlations are preliminary in nature since they rely on a simple description of the molecular orbitals associated with the Franck–Condon region electronic transitions and neglect phenomena like curve crossing effects and/or mixing of the electronic states that may play an important role in determining the actual product channels for each electronic transition.

Based on our current DFT results as well as previous molecular beam and ultrafast spectroscopy experimental results [11,12,16] we propose the following preliminary assignment for the CF_2I_2 absorption band in the ultraviolet region: the weak shoulder ~ 349 nm is assigned to nominally forbidden triplet transitions (likely due to $^3B_1$ transitions receiving some intensity from the close and intense $^1B_1$ transition), the 305 nm band is assigned to a strong $^1B_1$ transition, the 267 nm band is assigned to the $^1A_2$ and $^1B_2$ transitions, and the 248 nm band is assigned to the $^1A_1$ transition. The oscillator strengths computed for the 294 nm ($^1B_1$), 259 nm ($^1B_2$), and 250 nm ($^1A_1$) transitions are reasonably close to those derived from the gaussian deconvolution of the experimental spectrum of Fig. 1. The present assignments are somewhat different than those originally proposed for CF_2I_2 [12], but are not necessarily inconsistent with the experimental data and main results of these previous experiments [12]. We note that the majority of our DFT computational results (as well as the experimental resonance Raman spectra) appear consistent with the main findings of the previous CF_2I_2 experiments [11,12,16]. All of the work (including this study) on CF_2I_2 so far agrees that the largest transition ~ 305 nm has B_1 symmetry. The differing assignments for the ~ 349 and 248 nm regions could be due to a number of factors. First, several transitions are excited simultaneously and contribute to the anisotropy data which may make it difficult to extract these different contributions. For instance, the largest $^1B_1$ transition will still make a noticeable contribution to the 351 nm experimental data. In addition, the nominally forbidden triplet state transitions that are active ~ 349 nm could be the $^3B_1$ states (there are two above 300 nm). These states could conceivably pick up intensity from interaction with the nearby strong $^1B_1$ transition. This would be consistent with the molecular beam anisotropy results that indicate a B_1 symmetry transition [12]. Baum et al. [12] already noted that they needed to introduce some range of I–C–I bending motion into their recoil model to better fit their 248 nm TOF data. Examination of the resonance Raman spectra for both CH_2I_2 and CF_2I_2 reveals that there is a large amount of Franck–Condon activity in the I–C–I bending mode (ν_4) at most wavelengths and this implies that during the initial photodissociation the molecule changes its displacement in this mode significantly. This suggest that it may be useful to use a recoil model for the dissociation that takes into account the multidimensional nature of the reaction coordinate and the short-time dynamics. It also appears worth exploring to what extent the very large $^1B_1$ transition ~ 305 nm mixes with the nearby transitions. The transitions at wavelengths between 210 and 280 nm for CF_2I_2 are difficult to unambiguously assign due to severe overlap of several transitions and additional work is needed to resolve the apparent uncertainty in the 248 nm band assignment.

Further work that includes more sophisticated calculations and a variety of experimental techniques applied to the ultraviolet absorption band are needed to better understand the rich spectroscopy and photochemistry associated with the CF_2I_2 molecular system.

Acknowledgements

This work was supported by grants from the Committee on Research and Conference Grants (CRCG), the Research Grants Council (RGC) of Hong Kong, the Hung Hing Ying Physical Sciences

Research Fund and the Large Items of Equipment Allocation 1993–94 from the University of Hong Kong.

References

[1] M. Kawasaki, S.J. Lee, R. Bersohn, J. Chem. Phys. 63 (1975) 809.
[2] P.M. Kroger, P.C. Demou, S.J. Riley, J. Chem. Phys. 65 (1976) 1823.
[3] A. Gedanken, M.D. Rowe, Chem. Phys. 36 (1979) 181.
[4] S.L. Baughcum, H. Hofmann, S.R. Leone, D.J. Nesbitt, Faraday Discuss. Chem. Soc. 67 (1979) 306.
[5] S.L. Baughcum, S.R. Leone, J. Chem. Phys. 72 (1980) 6531.
[6] G. Schmitt, F.J. Comes, J. Photochem. 14 (1980) 107.
[7] H. Okabe, M. Kawasaki, Y. Tanaka, J. Chem. Phys. 73 (1980) 6162.
[8] J.B. Koffend, S.R. Leone, Chem. Phys. Lett. 81 (1981) 136.
[9] S.R. Cain, R. Hoffman, R. Grant, J. Phys. Chem. 85 (1981) 4046.
[10] C. Fotakis, M. Martin, R.J. Donovan, J. Chem. Soc., Faraday Trans. II 78 (1982) 1363.
[11] E.A.J. Wannenmacher, P. Felder, J.R. Huber, J. Chem. Phys. 95 (1991) 986.
[12] G. Baum, P. Felder, J.R. Huber, J. Chem. Phys. 98 (1993) 1999.
[13] B.J. Schwartz, J.C. King, J.Z. Zhang, C.B. Harris, Chem. Phys. Lett. 203 (1993) 503.
[14] K. Saitow, Y. Naitoh, K. Tominaga, K. Yoshihara, Chem. Phys. Lett. 262 (1996) 621.
[15] U. Marvet, M. Dantus, Chem. Phys. Lett. 256 (1996) 57.
[16] W. Radloff, P. Farmanara, V. Stert, E. Schreiber, J.R. Huber, Chem. Phys. Lett. 291 (1998) 173.
[17] J. Zhang, D.G. Imre, J. Chem. Phys. 89 (1988) 309.
[18] J. Zhang, E.J. Heller, D. Huber, D.G. Imre, D. Tannor, J. Chem. Phys. 89 (1988) 3602.
[19] W.M. Kwok, D.L. Phillips, Chem. Phys. Lett. 235 (1995) 260.
[20] W.M. Kwok, D.L. Phillips, J. Chem. Phys. 104 (1996) 2529.
[21] F. Duschek, M. Schmitt, P. Vogt, A. Materny, W. Kiefer, J. Raman Spectrosc. 28 (1997) 445.
[22] M. Braun, A. Materny, M. Schmitt, W. Kiefer, V. Engel, Chem. Phys. Lett. 284 (1998) 39.
[23] M.J. Frisch et al., GAUSSIAN 98, Revision A.7, Gaussian, Inc., Pittsburgh, PA, 1998.
[24] A.D. Becke, J. Chem. Phys. 98 (1993) 1372.
[25] R. Bauernschmitt, R. Ahlrichs, Chem. Phys. Lett. 256 (1996) 454.
[26] D.G. Imre, J.L. Kinsey, A. Sinha, J. Krenos, J. Phys. Chem. 88 (1984) 3956.
[27] G.E. Galica, B.R. Johnson, J.L. Kinsey, M.O. Hale, J. Phys. Chem. 95 (1991) 7994.
[28] K.Q. Lao, M.D. Person, P. Xayaroboun, L.J. Butler, J. Chem. Phys. 92 (1990) 823.
[29] F. Markel, A.B. Myers, J. Chem. Phys. 98 (1993) 21.
[30] P.G. Wang, L.D. Ziegler, J. Phys. Chem. 97 (1993) 3139.
[31] D.L. Phillips, A.B. Myers, J. Chem. Phys. 95 (1991) 226.
[32] D.L. Phillips, A.B. Myers, J. Raman Spectrosc. 28 (1997) 839.
[33] P. Venkateswarlu, Phys. Rev. 77 (1950) 676.
[34] S. Koda, Chem. Phys. Lett. 55 (1978) 353.
[35] J.C. Stephenson, D.S. King, J. Chem. Phys. 69 (1978) 1485.